

POLARIZATION

reveals the details

By Shuliang Jiao and

Lihong Wang, Texas A&M University

Optical coherence tomography (OCT) is an interferometric, noninvasive, noncontact imaging technology that can image biological tissues at micrometer-scale resolutions. Since it was first developed in 1991, the technique has become a major area of research in the field of biomedical optics with applications in ophthalmology, cardiology, neurology, gynecology, dermatology, dentistry, developmental biology, urology, and gastroenterology.

OCT detects the interference signal between the back-reflected probe light and the reference light passing through an interferometer. The depth resolution of OCT (1 to 10 μm) is determined by the source coherence length—interference occurs only when the optical path-length difference between the probe beam and reference beam is within the coherence length of the broadband light source. The lateral resolution, as in the case of confocal microscopy, is determined by the diameter of the focused probe beam in the sample. The imaging depth of the technique is limited to the quasi-ballistic regime (1 to 2 mm) in scattering biological tissues.

The contrast in an OCT image comes from the properties of the sample that modify the parameters of the probe light. Analogous to ultrasound B-mode imaging, OCT can image not only the microstructures of biological samples but also the blood flow. Unlike sound waves, however, light as a transverse wave has polarization, a property we can leverage to enhance contrast via polarization-sensitive OCT (PS-OCT).¹⁻³ This technique is important because polarization exists in many biological components such as collagen, retinal tissue, keratin, and myelin. Furthermore, highly birefringent collagen is ubiquitous in biological tissues, and its birefringence can be altered by denaturalization processes; therefore, these intrinsic polarization contrast mechanisms can be used as diagnostic indicators.

The parameters that characterize the polarization properties of a sample include birefringence and diattenuation, both of which can be described with their

By imaging birefringence in tissues,
polarization-sensitive Mueller-matrix
optical coherence tomography
reveals subsurface details in structure.



ILLUSTRATION BY PETER BENNETT

amplitudes, orientations, and ellipticities; for example, a waveplate can be described with its amplitude of retardation (for example, $\lambda/4$), the orientation of its fast axis (for example, 45°) and its ellipticity (for example, linear or circular). Birefringence is a description of the anisotropic dependence of the phase velocity of light in a sample on the incident polarization state; therefore, it provides polarization-based phase contrast. Diattenuation is a description of the dependence of intensity transmittance on the incident polarization state; therefore, it provides polarization-based amplitude contrast.

Mueller-matrix OCT

Mueller matrix and Jones matrix

In polarimetry, the polarization state of a light field can always be completely characterized by a Stokes vector (\mathbf{S}) and sometimes by a Jones vector (\mathbf{E}). A Stokes vector \mathbf{S} is constructed based on six flux measurements with different polarization analyzers in front of the detector: $\mathbf{S} = [S_0 \ S_1 \ S_2 \ S_3]^T = [I_H + I_V \ I_H - I_V \ I_P - I_M \ I_R - I_L]^T$, where S_0 – S_3 are the elements of \mathbf{S} , I_H , I_V , I_P , I_M , I_R , and I_L are the light intensities measured with a horizontal linear, a vertical linear, a $+45^\circ$ linear, a -45° linear, a right circular, and a left circular analyzer, respectively; the superscript T transposes a row vector into a column vector. A Jones vector comprises the horizontal and vertical components of the electric vector of the light field. It is suitable only for a pure polarization state—that is, one in which the degree of polarization is unity.

Correspondingly, the polarization properties of a sample

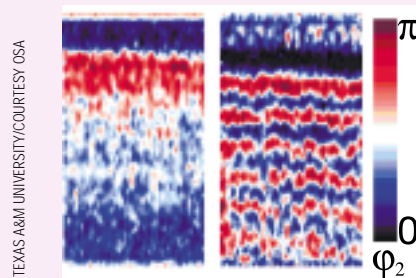


Figure 1 Compared to the measured backscattering image (M_{00} element of the Mueller matrix, left), the retardation image of a piece of porcine tendon shows bands that indicate birefringence. The height of the images is $750 \mu\text{m}$; the color bar indicates retardation.

polarization state $\mathbf{E}_{\text{out}} = \mathbf{J}\mathbf{E}_{\text{in}}$.

For a non-depolarizing sample, the Jones and Mueller matrices are equivalent and interchangeable. We have proved that even a scattering sample behaves as a non-depolarizing medium in OCT as a result of the coherent detection scheme.⁴ Consequently, either Jones or Mueller calculus can be used in OCT. Upon acquisition of the Mueller or Jones matrix, which can be provided by Mueller-matrix OCT, any polarization parameters can be extracted. We define a Mueller-matrix OCT system as a PS-OCT system that can measure the Mueller or Jones matrix of a sample. Mueller-matrix OCT is therefore the most general form of PS-OCT.

A Mueller matrix contains only real numbers, and the backscattering intensity transformation property of a sample is explicitly expressed in its M_{00} element. Accordingly, an M_{00} image provides the backscattering intensity contrast of a sample without being influenced by its polarization properties; a Mueller matrix thus clearly separates the backscattering structural information from the polarization information of a sample.

On the other hand, a Jones matrix has fewer elements, and its matrix elements can be interpreted more easily than those of a Mueller matrix. A Jones matrix has four complex elements in which one phase is arbitrary; therefore,

there are seven independent, real parameters in general, which are further reduced to five in OCT as a result of the transpose symmetry of a Jones matrix. The number of independent real components is the same in either the Jones matrix or its equivalent Mueller matrix. However, none of the elements in a Jones matrix plays the role of the M_{00} element in a Mueller matrix. In our experiments,

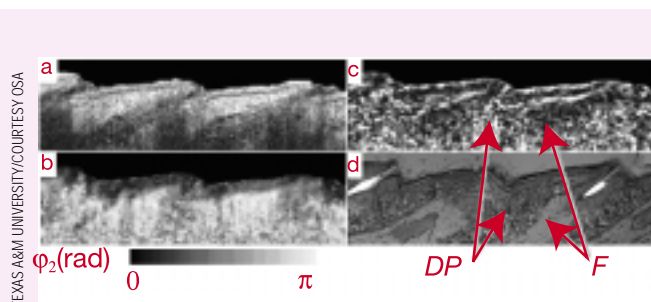


Figure 2 In this image of rat-tail tissue, the backscattering image reveals the boundaries of the structures in the epidermis and the shallow dermal region (a), while the retardation image shows components deeper in the dermis (b). The differential retardation image shows the birefringent regions comprising the collagen-rich dermal papillae (DP), as well as non-birefringent regions consisting of fat (F) and living epidermis (c). We include the polarization histologic image for comparison (d). The height of each image is $750 \mu\text{m}$; the gray scale is for the retardation (φ_2) image only.

can be completely characterized by a 4×4 Mueller matrix \mathbf{M} , which transforms the input Stokes vector \mathbf{S}_{in} into an output Stokes vector $\mathbf{S}_{\text{out}} = \mathbf{M}\mathbf{S}_{\text{in}}$. Likewise, a 2×2 complex Jones matrix can also be used to completely characterize the polarization properties of a sample if the sample is non-depolarizing—that is, a sample that transforms a pure input polarization state \mathbf{E}_{in} into a pure output

we first measure the Jones matrix and then transform it into the corresponding Mueller matrix to combine the advantages of the two approaches.

Multichannel Mueller-matrix OCT

Our group built a multichannel Mueller OCT system with a pair of superluminescent diodes (SLDs) that generate horizontally and vertically polarized emission, respectively. The SLDs operate at 850 nm with a 26-nm bandwidth. The two source beams, amplitude-modulated at different frequencies, are first merged by a polarizing beamsplitter and spatially filtered, then split by a non-polarizing beamsplitter into the reference arm and the sample arm. A 45° linear polarizer in the reference arm controls the polarization state of the reference beam.

A second polarizing beamsplitter divides the combined backscattered and reference light into horizontally and vertically polarized components—the components of the output Jones vectors. These components are coupled into single mode optical fibers and detected by photodiodes. A DC-motor-driven translation stage provides the depth scan.

Due to the mutual independence and differing modulation frequencies of the two light sources, the system produces two sets of interference signals with distinct carrier frequencies. The output Jones vectors corresponding to the two input polarization states can be constructed by filtering the interference signals, then performing a Hilbert transformation. After determining the output Jones vectors for the two independent incident polarization states, we can then calculate the Jones matrix.

imaging biological samples

We have used the multi-channel Mueller OCT system to image biological samples. The image of the calculated phase retardation for a piece of porcine tendon shows the birefringent properties of the collagen fibers in the tissue (see figure 1 on page 21). In comparison to the image of the M_{00} element of the Mueller matrix, the retardation image reveals clear stripe structures that are caused by the phase wrapping of the retardation over a range of $[0, \pi]$. The stripe structure distributes quite uniformly in the measured region, indicating the uniform birefringence in this area.

The system also revealed details in the skin of a Berlin Druce (BD-IV) rat tail (see figure 2 on page 21). The Jones matrix provided the polarization parameters of the sample. Both the M_{00} and retardation images reveal different characteristics of the tissue. Some structures, like the collagen-rich dermal papillae, can be clearly seen in both images. But while the M_{00} images clearly reveal the boundaries of the structures in the epidermis and the shallow dermal region, the retardation image reveals the distribution of the birefringent components deeper in the dermis. To obtain a differential retardation image,

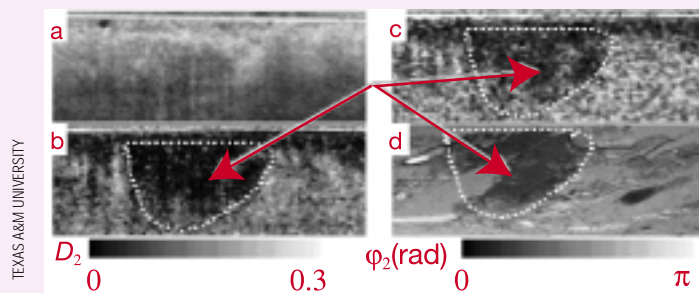


Figure 3 Compared to the intensity image (a), the retardation (b) and diattenuation (c), and polarization histologic images (d) of a burned region on a rat tissue sample clearly show the burn, which corresponds to a region of low birefringence and diattenuation. The height of each image is 750 μm . The gray scales are for the retardation (ϕ_2) and diattenuation (D_2) images, respectively.

we calculate the absolute value of the retardation difference between a given pixel and its previous pixel along the same longitudinal scan line. In comparison to the raw retardation image, this differential retardation image more clearly reveals the birefringent regions (corresponding to the superficial keratin layer and collagen-rich dermal papillae) and non-birefringent regions (corresponding to fat and the living epidermis).

To evaluate the efficacy of polarization contrast in burn-depth determination, we imaged an ex vivo rat-belly skin sample that contained a burn lesion (see figure 3). The burn region cannot be identified in the intensity image, but it can be clearly seen with marked contrast in the retardation and diattenuation images. The loss of birefringence and diattenuation in the burn region is caused by the thermally induced coagulation of the collagen fibers. The polarization histological image confirms the size and location of the burn region.

From the experimental results, we can see that the polarization properties of biological tissues offer sensitive contrast mechanisms for monitoring tissue functional conditions. Because it can provide comprehensive structural and polarization information, multichannel Mueller-matrix OCT has a variety of potential medical applications, such as in the diagnosis of burns and glaucoma. **oe**

Shuliang Jiao is a PhD candidate and Lihong Wang is a professor and director at the Optical Imaging Laboratory,

Department of Biomedical Engineering, Texas A&M University, College Station, TX. For questions about this article, contact Wang at 979-847-9040 (phone), 979-845-4450 (fax), or LWang@tamu.edu (e-mail).

References

1. J. de Boer, T. Milner, et al., *Opt. Lett.* 22, 934-936 (1997).
2. S. Jiao and L. Wang, *Opt. Lett.* 27, 101-103 (2002).
3. S. Jiao, W. Yu, et al., *Opt. Lett.* in press (2003).
4. S. Jiao, G. Yao, et al., *Appl. Opt.* 39, 6318-6324 (2000).